Microchimica Acta (2018) 185: 92
https://doi.org/10.1007/s00604-017-2651-z

ORIGINAL PAPER

A conventional chemical reaction for use in an unconventional assay: A colorimetric immunoassay for aflatoxin B_1 by using enzyme-responsive just-in-time generation of a MnO_2 based nanocatalyst

Wenqiang Lai[1] · Qiao Zeng[2] · Juan Tang[3] · Maosheng Zhang[1] · Dianping Tang[4]

Received: 23 October 2017 / Accepted: 29 December 2017 / Published online: 10 January 2018

Abstract

The authors describe a colorimetric immunoassay for the model nalyte aflatoxin B_1 (AFB_1). It is based on the just-in-time generation of an MnO_2 nanocatalyst. Unlike previously developed immunoassay, the chromogenic reaction relies on the just-in-time formation of an oxidase mimic without the aid of the substrate. Potassium permanganate ($KMnO_4$) is converted into manganese dioxide (MnO_2) which acts as an oxidase mimic that catalyzes the oxidation 3,3′,5,5′-tetramethylbenzidine (TMB) by oxygen to give a blue colored product. In the presence of ascorbic acid (AA), $KMnO_4$ is reduced to Mn(II) ions. This results in a decrease in the amount of MnO_2 nanocatalyst. Hence, the oxidation of TMB does not take place. By adding ascorbate oxidase, AA is converted into dehydroascorbic acid which cannot reduce $KMnO_4$. Based on these observations, a colorimetric competitive enzyme immunoassay was developed where ascorbate oxidase and gold nanoparticle-labeled antibody against AFB_1 and magnetic beads carrying bovine serum albumin conjugated to AFB_1 are used for the determination of AFB_1. In presence of AFB_1, it will compete with the BSA-conjugated AFB_1 (on the magnetic beads) for the labeled antibody against AFB_1 on the gold nanoparticles. This makes the amount of ascorbate oxidase/anti-AFB_1 antibody-labeled gold nanoparticles, which conjugated on magnetic beads, reduce, and resulted in an increase of ascorbic acid. Under optimal conditions, the absorbance (measured at 652 nm) decreases with increasing AFB_1 concentrations in the range from 0.1 to 100 ng mL^{-1}, with a 0.1 ng mL^{-1} detection limit (at the $3S_{blank}$ level). The accuracy of the assay was validated by analyzing spiked peanut samples. The results matched well with those obtained with a commercial ELISA kit. Conceivably, the method is not limited to aflatoxins but has a wide scope in that it may be applied to many other analytes for which respective antibodies are available.

Electronic supplementary material The online version of this article (https://doi.org/10.1007/s00604-017-2651-z) contains supplementary material, which is available to authorized users.

✉ Wenqiang Lai
wenqiang.lai@mnnu.edu.cn

[1] Key Laboratory of Modern Analytical Science and Separation Technology, College of Chemistry and Environment, Minnan Normal University, Zhangzhou 363000, People's Republic of China

[2] Ji'an Vocational Polytechnic College, Ji'an 343000, People's Republic of China

[3] Ministry of Education Key Laboratory of Functional Small Organic Molecule, Department of Chemistry and chemical engineering, Jiangxi Normal University, Nanchang 330022, People's Republic of China

[4] Key Laboratory of Analysis and Detection for Food Safety (Ministry of Education & Fujian Province), Institute of Nanomedicine and Nanobiosensing, Department of Chemistry, Fuzhou University, Fuzhou 350108, People's Republic of China

Keywords Just-in-time generation · Colorimetric immunoassay · Aflatoxin B_1 · Enzyme cascade amplification · UV-vis adsorption spectroscopy · Cuvette · Microtiter plate · Naturally contaminated/spiked food sample

Introduction

Aflatoxins, the highly toxic secondary metabolites produced by a number of different fungi, are present in a wide range of food and feed commodities, and are assumed significant because of their deleterious effects on human beings, poultry, and livestock [1–6]. The major aflatoxins of interest are designated as B_1, B_2, G_1, and G_2; however, aflatoxin B_1 (AFB_1) is usually predominant and the most hazardous [7]. Thus, exploring validated analytical methods for rapid detection of AFB_1 on a large scale is important. Thereinto, colorimetric immunoassays achieve the great efforts in the application of

the determination of various biomakers [8, 9]. Based on different signal-generation principles, enzyme-based colorimetric immunoassay is usually employed to realize this purpose because of its simplicity, general applicability, and high-speed operation [10, 11]. The commercialization of enzyme-linked immunosorbent assay kit expands the application prospect of the method. Despite some advances in this field, there is still the request for exploiting new immunoassay schemes in order to keep pace with expectations in future testing.

For traditional colorimetric immunoassays, there are usually two models to be used. One method is to use the dispersion and aggregation of nanoparticles [*e.g.*, gold nanoparticles (AuNP) and silver nanoparticles] to produce the change in the color for the quantitative monitoring [12–14]. Another strategy is to oxidize the chromogenic agents [*e.g.*, 3,3′,5,5′-tetramethylbenzidine, TMB; o-phenylenediamine and 2,2′-azinobis-(3-ethylbenzthiazoline-6-sulphonate)] through natural enzymes or enzyme mimics [15–17]. Both protocols have had enough efforts and quite mature. As we know, unfortunately, the methods are still subjected to some restriction such as the synthesis and stockpile of nanomaterials. As time goes on, that is, the surface character of nanoparticles will be changed and resulted in the change of the catalytic activity. After careful search, there is no report focusing on just-in-time generation (*i.e.*, synthesis in a very short period of time) of enzymatic nano-mimics to solve the issue of maintaining activity. Gao et al. used ascorbic acid (AA), produced catalytically by alkaline phosphatase (ALP), to reduce H_2PdCl_6 on AuNP as peroxidase mimic, which could catalyze TMB-H_2O_2 system to produce colored products [18]. Despite the high sensitivity of the assay, it has limitations. In the process of synthesis of nanoparticle mimic, one supporter (*i.e.*, AuNP) is needed. So, finding one just-in-time enzyme mimic without supporter should be worth of focusing on nowadays.

Currently, the synthesis of most materials almost needs to spend certain period of time and/or other rigorous conditions (*e.g.*, temperature or solvent) [19–22]. In contrast, the relatively simple materials (*e.g.*, AuNP) also need several quarters. Herein, it is very necessary for the research about just-in-time generation of the materials. Manganese (Mn) possesses a variety of valence state, ensuring that a variety of manganese materials with different valence state are synthesized easily. We found that manganese dioxide (MnO_2) could be synthesized directly through the reaction between potassium permanganate ($KMnO_4$) and Mn(II) without complicated synthesis and the requirement of temperature. Moreover, MnO_2, applied in different field widely, exhibits oxidase activity and could catalyze chromogenic agent to produce a color change in the absence of H_2O_2 [23–25]. Therefore, the synthetic route of nanomaterials by just-in-time generation strategy, which could catalyze chromogenic agent simultaneously, is possible. Compared to using $KMnO_4$ alone, the generation of MnO_2 via $KMnO_4$ can improve the sensitivity of the detection. On the other hand, reducing agent (*e.g.*, ascorbic acid, AA; glutathione, GSH) can chemically reduce $KMnO_4$ and MnO_2, thus resulting in the loss of peroxidase-like activity or oxidase-like activity [26]. When equivalent AA reduces equivalent MnO_2 to Mn(II), the diminishing portion of MnO_2 can influence multiple of oxidization of TMB, resulted in the improving of sensitivity. Typically, dehydroascorbic acid (DAA) can be generated by ascorbate oxidase (AOx) toward the catalytic oxidation of AA. Such a cascade reaction system can result in the signal amplification on several orders of magnitude within milliseconds. In this case, AA-controlled chemical conversion of MnO_2 to Mn(II) can be utilized for quantitatively monitoring of AOx activity.

In this study, we exploited a novel colorimetric platform based on just-in-time generation of MnO_2 oxidase mimic. The platform was applied in colorimetric immunoassay for detection of aflatoxin B_1 (AFB_1 as a model analyte) based on AOx-labeled immunogold as the signal-transduction tag with a competitive-type immunoassay format (Scheme 1). In the presence of target AFB_1, the carried AOx initially catalyzes AA to DAA, and hinder to reduce $KMnO_4$, thereby increasing of generated MnO_2. Then the solution can display a blue color. By monitoring the change in the visible color or absorbance, we can qualitatively or quantitatively determine the concentration of target AFB_1 in the sample.

Experimental

Material and reagents

Monoclonal anti-AFB_1 antibody (mAb 62, clone 2B7) was obtained from Tang's scientific partner (Dietmar Knopp, Chair for Analytical Chemistry, Institute of Hydrochemistry, Technische Universität München, Germany; www.ws.chemie.tumuenchen.de). AFB_1 standards from *Aspergillus flavus* (product no.: A6636) and AOx were purchased from Sigma-Aldrich (Shanghai, China, www. sigmaaldrich.com). AFB_1-BSA conjugate was gifted from the School of Food Science and Technology, Jiangnan University (Wuxi, China). 3,3′,5,5'-Tetramethylbenzidine (TMB) and BSA were achieved from Sinopharm Chem. Re. Co., Ltd. (Shanghai, China, www.sinopharm.com). $KMnO_4$ and $MnSO_4$ were obtained from Fuchen Chemicals (Tianjin, China, www.tjfch.com). All other reagents were used as received without further purification. All water used in this work was of Milli-Q ultrapure grade (EMD Millipore, www.merckmillipore.com). In the preparation of a carbonate buffer of pH 9.6, Na_2CO_3 (1.59 g) and $NaHCO_3$ (2.93 g) were dissolved in 1000 mL distilled water. A pH 6.5 phosphate-buffered (PBF, 0.5 mM) were prepared by mixing definite volumes of 0.5 mmol L^{-1} Na_2HPO_4•$12H_2O$ and 0.5 mmol L^{-1} NaH_2PO_4. PBF (pH 7.4) was prepared by using 2.9 g Na_2HPO_4, 0.24 g KH_2PO_4, 0.2 g

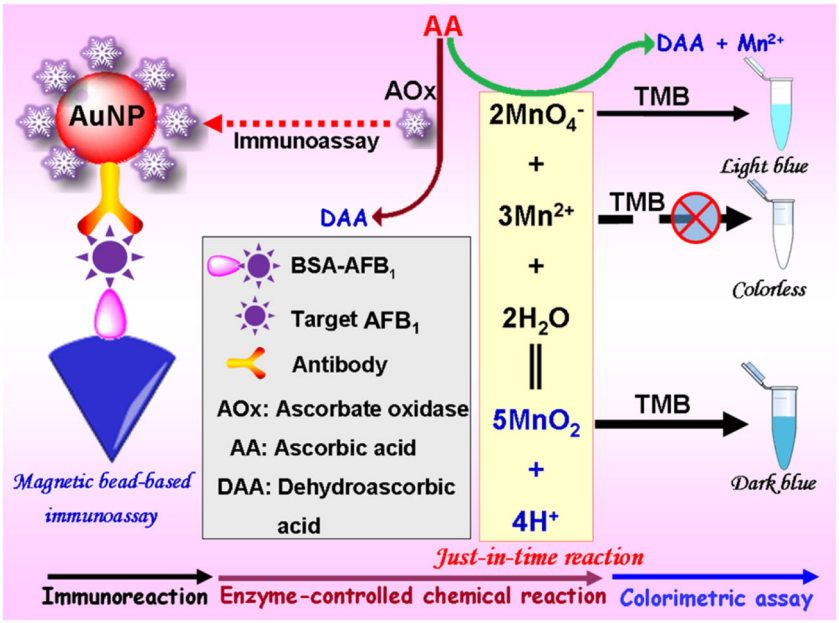

Scheme 1 Schematic illustration of conventional chemical reaction for unconventional application in the magnetically responsive colorimetric immunoassay using enzyme-responsive just-in-time generation of MnO_2 nanocatalyst

KCl and 8.0 g NaCl in 1000 mL distilled water. The washing and blocking buffers were obtained by adding 0.05% Tween 20 (*v*/v) and 0.1 wt% BSA in PBF, respectively.

Monitoring of AOx activity based on just-in-time generation of oxidase mimic

Scheme 1 displays the detection principle of AOx activity based on just-in-time generation of oxidase mimic. The assay was carried out as follows: (i) 10 μL of AOx with different concentrations (from 0 to 1000 mU mL^{-1}) was added into 50 μL of PBF (pH 6.5) containing 200 μM AA and incubated for 15 min at room temperature (RT); (ii) 10 μL of 1 mM $KMnO_4$ and 10 μL of 2 mM $MnSO_4$ were injected into the resulting solution and reacted for 1 min at RT; and (iii) 100 μL of 1 mM TMB substrate solution (ethanol: buffer = 1: 9) in pH 4.0 citrate acid-disodium hydrogen phosphate buffer was injected and incubated for 2 min at RT. The resultant mixture was monitored on a microplate reader (Tecan Infinite 200 PRO, TECAN, Switzerland www.tecan.com), and the absorbance was recorded at λ = 652 nm.

Colorimetric immunoassay toward AFB_1 based on enzyme-controlled just-in-time generation of oxidase mimic

Scheme 1 gives the monitoring process of colorimetric immunoassay toward target AFB_1 based on enzyme-controlled just-in-time generation of oxidase mimic. AFB_1-BSA-conjugated magnetic bead (designated as AFB_1-MB) and mAb/AOx-Labeled gold Nanoparticle (*i.e.*, mAb-AuNP-AOx) are prepared according to our previous report with minor modification [15]. Initially, 25 μL of AFB_1 standard/sample and 50 μL of mAb-AuNP-AOx suspension were added in sequence to 25 μL of AFB_1-MB suspension (6 mg mL^{-1}) in a 200-μL PCR tube, and incubated for 60 min at 37 °C (adequately reaction) with gentle shaking. After that, the resulting suspension was collected by using an external magnet and washed with the washing buffer. 50 μL of 200 μM AA (pH 6.5 PBF) was added to the precipitate and incubated for 15 min at RT. Following that, 10 μL of 1 mM $KMnO_4$, and 10 μL of 2 mM $MnSO_4$ were injected into the mixture in turn as before. Finally, 100 μL of 1 mM TMB substrate solution was added and incubated for 2 min for color development. The absorbance was registered and recorded at λ = 652 nm on a plate reader.

Results and discussion

Design of just-in-time generation of oxidase mimic-based colorimetric immunoassay

Based on high catalytic activity of enzyme, oxidase possesses much stronger efficiency than the equivalent of oxidizer toward chromogenic agent. So, the assumption if oxidizer (*e.g.*, $KMnO_4$) can turn into oxidase mimic (*e.g.*, MnO_2) is carried out to achieve the goal of signal amplification. To ensure the feasibility of the idea, the choice of $KMnO_4$-to-MnO_2 was attempted (Fig. 1A). As shown in curve '*b*' and curve '*c*' in Fig. 1A, no absorbance peak is observed, stated that no effect of Mn(II) toward TMB. When $KMnO_4$ is added, the absorbance peak at 652 nm is found on the basis of strong oxidizing of $KMnO_4$ (curve 'a' in Fig. 1A). Significantly, the absorbance has obvious increase with the adding of $KMnO_4$ and $MnSO_4$ simultaneously (curve '*d*' in Fig. 1A). The results

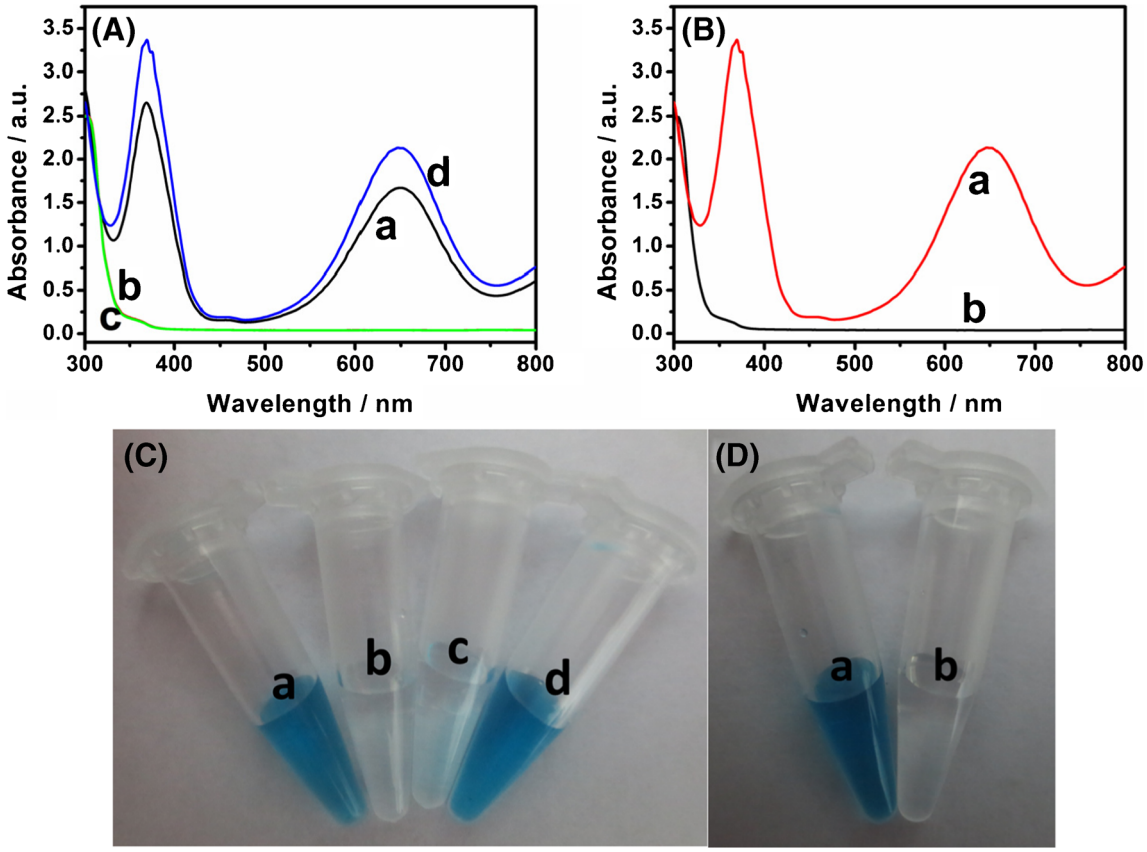

Fig. 1 **A** UV-vis absorption spectra and (**C**) photographs of (a) $KMnO_4$ + TMB, (b) Mn(II) + TMB, (c) TMB and (d) $KMnO_4$ + Mn(II) + TMB, respectively; **B** UV-vis absorption spectra and (**D**) photographs of (a) $KMnO_4$ + Mn(II) + TMB and (b) AA + $KMnO_4$ + Mn(II) + TMB, respectively (Note: 1.0 mM $KMnO_4$, 1.0 mM TMB, 1.0 mM AA and 2.0 mM Mn(II) used in all the cases)

prove the feasibility of oxidizer-to-oxidase mimic, and the method of just-in-time generation of oxidase mimic open a new situation for colorimetric assay. Then, we need to verity that the platform could be applied to colorimetric assay. In the presence of AA (curve '*b*' in Fig. 1B), the absorbance is decreased, thereby resulting in the change of the color (Fig. 1B). It insured scalability of the colorimetric platform, and could be applied effectively and widely.

The most important concern on our design is whether the choice of $KMnO_4$-to-MnO_2 could improve the sensitivity and detection limit (LOD) in colorimetric assay. To verify this point, Fig. 2A shows the effect of various concentrations AA toward $KMnO_4$ and $KMnO_4$-Mn(II) system, respectively ($n = 3$). The absorbance decreases with increasing AA concentration. As shown in Fig. 2B, what's more, we find that the $KMnO_4$-Mn(II) system has more sensitive response than the

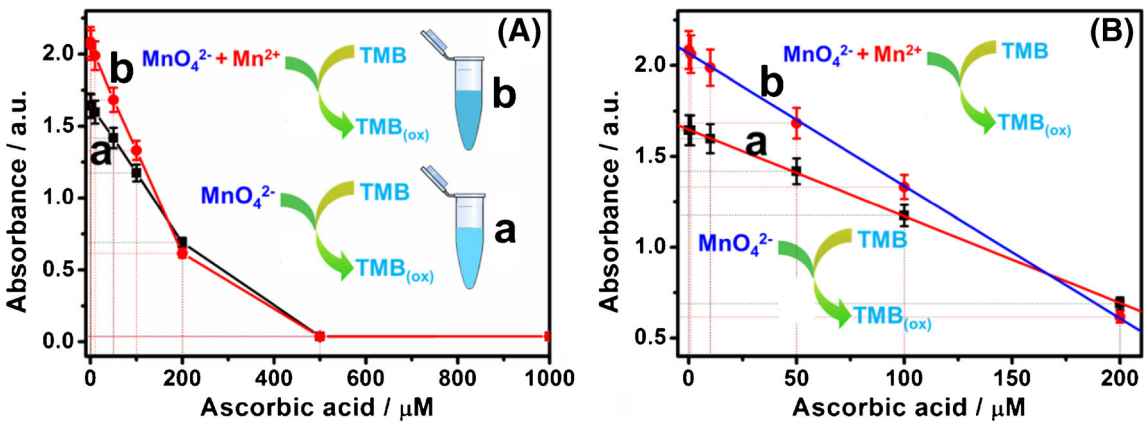

Fig. 2 **A** Comparison of (a) TMB + $KMnO_4$ and (b) TMB + $KMnO_4$ + Mn(II) towards different-concentration ascorbic acid standards in the absorbance, and (**B**) the corresponding linear plots of Fig. A

$KMnO_4$. The LOD (1.0 μM) of the $KMnO_4$-Mn(II) system is lower than that (10 μM) of the $KMnO_4$. The results prove that just-in-time generation of oxidase mimic through oxidizer was of great significance for development of colorimetric assay.

Control tests for just-in-time generation of MnO_2-based colorimetric system

Ascorbate oxidase (AOx) could be applied in oxidation of AA for a stabilizer. So, the colorimetric platform was used in this work for detection of AOx activity. Initially, we investigate several control tests under the different conditions (Fig. 3). When AOx, AA, $KMnO_4$, $MnSO_4$, and TMB is all added into solution, two obvious absorption peaks at 652 and 372 nm would are found (curve '*a*'). When AOx is absent (curve '*b*'), the absorbance is decreased, and stated the effect of AOx toward AA. When AA is absent (curve '*c*'), two higher absorbance peak is appeared in comparison to curve '*a*'. The result shows that AA could decrease absorbance. When $KMnO_4$ (curve '*d*') or TMB (curve '*f*') are absent, no absorbance peak is existent, and verified that $MnSO_4$ could not catalyze TMB, the origin of the color, and produce color change. When $MnSO_4$ is absent (curve '*e*'), the absorbance is a bit lower than curve '*a*'. It explains that just-in-time generation's method could amplify signal. The whole result well expounds the process of the colorimetric platform toward AOx. Following that, the enzymatic reactivity of AOx in colorimetric platform was also studied. As shown in Fig. S4, the absorbance increases with increasing AOx concentration, and the LOD is ~ 15 mU mL^{-1} AOx.

Optimization of experimental conditions

In the case of 1.0 mM $KMnO_4$ and 2.0 mM $MnSO_4$, the reaction time toward TMB was optimized (Fig. S1). The reaction is very fast, and reached to the steady-state equilibrium within two minute. So, 2 min is chosen for the colorimetric development in this work. Based on this data, we investigated the effect of $MnSO_4$ with various concentrations under the condition of 1.0 mM $KMnO_4$ and 1 mM TMB substrate solution (Fig. S2). The absorbance rapidly increases before 2.0 mM $MnSO_4$, and slowly tended to level off. Herein, we choose 2.0 mM $MnSO_4$ for the development of colorimetric platform. Following that, the reaction time and enzymatic reactivity of AOx in colorimetric platform were also studied. As shown in Fig. S3, 15 min is chosen because of the minute change after 15 min.

Analytical performance of the colorimetric immunoassay

The colorimetric platform could be applied to immunoassay. We used detection antibody and AOx-labeled gold nanoparticle (mAb-AuNP-AOx) as the signal-transduction tag and AFB_1-BSA-conjugated magnetic bead (AFB_1-MB) as the colorimetric platform with a competitive-type immunoassay format. As shown from Fig. 4A, the absorbance (λ = 652 nm) decreases with the increasing AFB_1 concentration in the sample. A good linear dependence between the absorbance and AFB_1 level could be acquired in the dynamic range from 0.1 to 100 ng mL^{-1}. The linear regression equation could be fitted to $y = -0.0051 \times C_{[AFB1]} + 1.1675$ (ng mL^{-1}, $R^2 = 0.9983$, $n = 6$). The LOD could be estimated to 0.1 ng mL^{-1} at the $3s_{blank}$ criterion, and meet the requirement of legal limit of AFB_1 in foodstuff (< 2.0 ng mL^{-1}) [27]. To further clarify the advantages of the immunoassay, the analytical properties were compared with other AFB_1 detection schemes (Table S1 in the Supporting Information). Apparently, the sensitivity (*i.e.*, LOD) is comparable to that of other methods. Although the LOD was somewhat higher than those of some methods (*e.g.*, electrochemical immunoassays and fluorescence immunoassays), this system is relatively low cost, and does not need

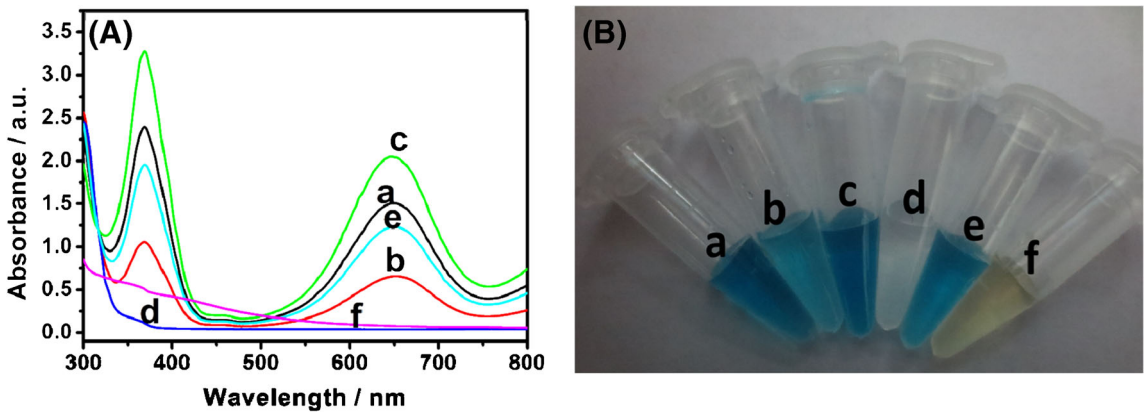

Fig. 3 **A** UV-vis absorption spectra of (a) AA + AOx + $KMnO_4$ + Mn(II) + TMB, (b) AA + $KMnO_4$ + Mn(II) + TMB, (c) AOx + $KMnO_4$ + Mn(II) + TMB, (d) AA + AOx + Mn(II) + TMB, (e) AA + AOx + $KMnO_4$ + TMB and (f) AA + AOx + $KMnO_4$ + Mn(II), respectively; and (**B**) the corresponding photographs for figure 'A'

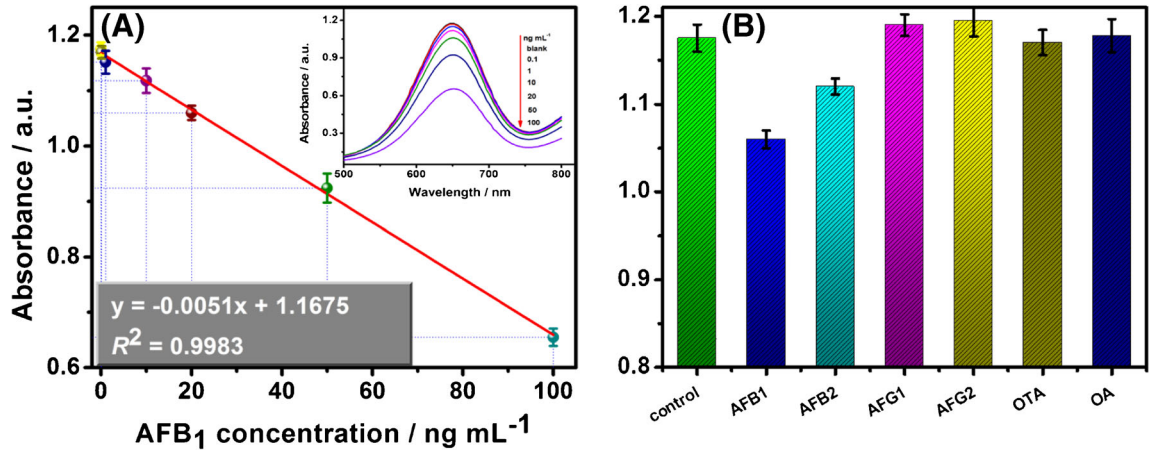

Fig. 4 **A** Calibration plots of unconventional competitive-type colorimetric immunoassay toward different-concentration AFB_1 standards (*Inset*: the corresponding UV-vis absorption spectra), and (**B**) specificity of our developed strategy toward target AFB_1 (20 ng mL^{-1}), AFB_2 (20 ng mL^{-1}), AFG_1 (20 ng mL^{-1}), AFG_2 (20 ng mL^{-1}), OTA (20 ng mL^{-1}) and OA (20 ng mL^{-1})

expensive instrumentations and complex operation. We also investigated the reproducibility and precision of the immunoassay toward 0.5 ng mL^{-1}, 50 ng mL^{-1} and 100 ng mL^{-1} AFB_1, respectively. The relative standard deviations (RSD) were 9.8%, 8.9% and 8.7% ($n = 3$), respectively, suggested that the reproducibility and precision of the colorimetric immunoassay were acceptable.

Further, we examined the specificity of the colorimetric immunoassay for target AFB_1 and other toxins, *e.g.*, aflatoxin B_2 (AFB_2), aflatoxin G_1 (AFG_1), aflatoxin G_2 (AFG_2), ochratoxin A (OTA) and okadaic acid (OA). As shown from Fig. 4B and Fig. S5, the absorbance obtained from AFG_1, AFG_2, OTA, and OA alone were almost the same as the background signal except for AFB_2. The reason might be attributed to the fact that anti-AFB_1 antibody used in this work has a high cross-reactivity with AFB_2, thus resulting in the change in the absorbance. The results clearly revealed that the specificity of the colorimetric immunoassay was acceptable.

Monitoring of real peanut samples

Finally, the colorimetric immunoassay for AFB_1 real samples was compared with a commercialized AFB_1 ELISA kit (Diagnostic Automation Inc.). AFB_1-spiked peanut standards and naturally contaminated peanut samples with various concentrations were prepared referring to our previous report [28]. For AFB_1-spiked peanut standards, firstly, a Midea Food Mixer (BP252AG, Guangdong, China) was used to extract the milled blank peanut sample (5.0 g) with the aid of 37.5 mL MeOH/water (80: 20, v:v). Following that, stirred for 60 min at RT and filtration were carried out. Then, the extract (20 mL) of 20% (*v*/v) MeOH was acquired toward to the

Table 1 Comparison of the results obtained by the colorimetric immunoassay and commercial AFB_1 ELISA Kit (Diagnostic Automation Inc., LOD = 5.0 pg mL^{-1}) for spiked or naturally contaminated peanut samples

Type	No.	Method; concentration (ng mL^{-1}, mean ± SD, $n = 3$)[a]		t_{exp}
		Colorimetric immunoassay [a]	AFB_1 ELISA kit	
Spiked peanut	1	17.5 ± 1.6	16.7 ± 0.9	0.75
	2	1.4 ± 0.2	1.8 ± 0.2	2.45
	3	0.71 ± 0.1	0.88 ± 0.08	2.30
	4	51.2 ± 2.0	49.3 ± 1.6	1.28
	5	0.23 ± 0.1	0.17 ± 0.2	0.46
Naturally contaminated peanut	6	6.2 ± 1.3	7.8 ± 0.9	1.75
	7	11.2 ± 0.7	11.8 ± 0.6	1.12
	8	89.7 ± 1.9	93.2 ± 2.4	1.98
	9	9.7 ± 0.8	8.7 ± 0.4	1.93
	10	76.3 ± 1.5	74.1 ± 1.1	2.05

[a] Each sample was determined in triplicate, and the high-concentration AFB_1 sample was assayed with an appropriate dilution. The linear regression equation for these usable mean data between two methods is as follows: $y = 1.0034\times - 0.0587$ ($R^2 = 0.9975$, $n = 10$; *x* axis: by the colorimetric immunoassay; *y* axis: by AFB_1 ELISA kit

addition of 60 mL ultrapure water. Finally, standard samples were prepared by spiking AFB_1 standards into different-volume diluted extract. For naturally contaminated peanut samples, 7.5 g of peanut slurry was extracted with 18 mL MeOH. Then, the contaminated peanut samples were obtained by addition of 15 mL ultrapure water into 5 mL extract. All data are summarized in Table 1. As shown in Table 1, all the results of t_{exp} were lower than t_{crit} ($t_{crit[4,\ 0.05]} = 2.77$). The regression equation (linear) could be fitted to $y = 1.0034\times - 0.0587$ ($R^2 = 0.9975$, $n = 10$). The results indicated that the colorimetric immunoassay could be regarded as an optional scheme for the monitoring of target AFB_1 in the complex systems.

Conclusions

In conclusion, this works reports a novel colorimetric detection method based on a classical chemical reaction for extraordinary application in the immunoassay. The just-in-time generation of MnO_2 peroxidase mimics via the reaction between MnO_4^- and Mn^{2+} could exhibit high catalytic activity toward TMB. In the presence of AOx, the chemical reaction could be controlled to carry out the signal change. Compared with traditional enzyme-based colorimetric immunoassays, the developed colorimetric platform was novel and rapid. More importantly, just-in-time generation of MnO_2 peroxidase mimic avoids much complex questions with preparing nanomaterial, opens a new situation for the development of colorimetric assay. The system is suitable for application in the clinical devices, even possible to realize the commercialization. Nevertheless, only one disadvantage of the developed strategy involved in strong oxidizing property of $KMnO_4$ itself, which might influence the LOD of the immunoassay. To fulfill the potential application for point-of-care testing, future work should focus on the improvement of sensitivity.

Acknowledgements Support by the National Natural Science Foundation of China (Grants No. 21505060), the Outstanding Youth Science Foundation of Fujian Province (Year 2017), the Program for Excellent Talents of Minnan Normal University (Grant No. MJ1601), the Natural Science Foundation of Zhangzhou City, China (Grant No. ZZ2016J30), the National Science Foundation of Fujian Province (Grant No. 2014 J07001).

Compliance with ethical standards The authors declare that they have no competing interests.

References

1. Abbas H, Accinelli C, Shier W (2017) Biological control of aflatoxin contamination in U.S. crops and the use of bioplastic formulations of aspergillus flavus biocontrol strains to optimize application strategies. J Agric Food Chem 65:7081–7087
2. Qi D, Fei T, Liu H, Yao H, Wu D, Liu B (2017) Development of multiple heart-cutting two-dimensional liquid chromatography coupled to quadrupole-orbitrap high resolution mass spectrometry for simultaneous determination of Aflatoxin B_1, B_2, G_1, G_2, and ochratoxin A in snus, a smokeless tobacco product. J Agric Food Chem 65:9923–9929
3. Lim C, Yomoya T, Layne J, Chan S (2015) Multi-mycotoxin screening reveals separate occurrence of aflatoxins and ochratoxin A in Asian rice. J Agric Food Chem 63:3104–3113
4. Li X, Yang F, Wong J, Yu H (2017) Integrated smartphone-app-chip system for on-site parts-per-billion-level colorimetric quantitation of aflatoxins. Anal Chem 89:8908–8916
5. Du B, Su X, Yang K, Pan L, Liu Q, Gong L, Wang P, Yang J, He Y (2017) Antibody-free colorimetric detection of total aflatoxins in rice based on a simple two-step chromogenic reaction. Anal Chem 89:4809–4815
6. Xie J, Jiang H, Shen J, Peng T, Wang J, Yao K, Sun S, Shao B, Tang J (2017) Design of multifunctional nanostructure for ultrafast extraction and purification of aflatoxins in foodstuffs. Anal Chem 89: 10556–10564
7. Zitomer N, Rybak M, Li Z, Walters M, Holman M (2015) Determination of aflatoxin B_1 in smokeless tobacco products by use of UHPLC-MS/MS. J Agric Food Chem 63:9131–9138
8. Eltzov E, Marks R (2017) Colorimetric stack pad immunoassay for bacterial identification. Biosens Bioelectron 87:572–578
9. Gao Z, Xu M, Hou L, Chen G, Tang D (2017) High-index {*hk*0} faceted platinum concave nanocubes with enhanced peroxidase-like activity for an ultrasensitive colorimetric immunoassay of the human prostate-specific antigen. Analyst 142:911–917
10. Lai W, Wei X, Zhuang J, Lu M, Tang D (2016) Fenton reaction-based colorimetric immunoassay for sensitive detection of brevetoxin B. Biosens Bioelectron 80:249–256
11. Fu X, Chen L, Choo J (2017) Optical nanoprobes for ultrasensitive immunoassay. Anal Chem 89:124–137
12. Liu Y, Zhang L, Wei W, Zhao H, Zhao Z, Zhang Y, Liu S (2015) Colorimetric detection of influenza A virus using antibody-functionalized gold nanoparticles. Analyst 140:3989–3995
13. Xu S, Ouyang W, Xie P, Lin Y, Qiu B, Lin Z, Chen G, Guo L (2017) Highly uniform gold nanobipyramids for ultrasensitive colorimetric detection of influenza virus. Anal Chem 89:1617–1623
14. Ma X, Chen Z, Kannan P, Lin Z, Qiu B, Guo L (2016) Gold nanorods as colorful chromogenic substrates for semiquantitative detection of nucleic acids, proteins, and small molecules with the naked eye. Anal Chem 88:3227–3234
15. Lai W, Zhuang J, Tang D (2015) Novel colorimetric immunoassay for ultrasensitive monitoring of brevetoxin B based on enzyme-controlled chemical conversion of sulfite to sulfate. J Agric Food Chem 63:1982–1989
16. Gao Z, Xu M, Hou L, Chen G, Tang D (2013) Irregular-shaped platinum nanoparticles as peroxidase mimics for highly efficient colorimetric immunoassay. Anal Chim Acta 776:79–86
17. Liu M, Jia C, Jin Q, Lou X, Yao S, Xiang J, Zhao J (2010) Novel colorimetric enzyme immunoassay for the detection of carcinoembryonic antigen. Talanta 81:1625–1629
18. Gao Z, Hou L, Xu M, Tang D (2014) Enhanced colorimetric immunoassay accompanying with enzyme cascade amplification strategy for ultrasensitive detection of low-abundance protein. Sci Rep 4:3966
19. Hu Y, Cheng H, Zhao X, Wu J, Muhammad F, Lin S, He J, Zhou L, Zhang C, Deng Y, Wang P, Zhou Z, Nie S, Wei H (2017) Surface-enhanced raman scattering active gold nanoparticles with enzyme-mimicking activities for measuring glucose and lactate in living tissues. ACS Nano 11:5558–5566
20. Lai W, Wei Q, Xu M, Zhuang J, Tang D (2017) Enzyme-controlled dissolution of MnO_2 nanoflakes with enzyme cascade amplification for colorimetric immunoassay. Biosens Bioelectron 89:645–651

21. Li H, Liu H, Zhang J, Cheng Y, Zhang C, Fei X, Xian Y (2017) Platinum nanoparticle encapsulated metal-organic frameworks for colorimetric measurement and facile removal of mercury(II). ACS Appl Mater Interfaces 9:40716–40725
22. Zhang C, Tang J, Huang L, Li Y, Tang D (2017) In-situ amplified voltammetric immunoassay for ochratoxin A by coupling a platinum nanocatalyst based enhancement to a redox cycling process promoted by an enzyme mimic. Microchim Acta 184:2445–2453
23. Yan X, Song Y, Wu X, Zhu C, Su X, Du D, Lin Y (2017) Oxidase-mimicking activity of ultrathin MnO_2 nanosheets in colorimetric assay of acetylcholinesterase activity. Nano 9:2317–2323
24. Pal J, Pal T (2016) Enzyme mimicking inorganic hybrid Ni@MnO_2 for colorimetric detection of uric acid in serum samples. RSC Adv 6:83738–83747
25. Lin L, Shi D, Li Q, Wang G, Zhang X (2016) Detection of T4 polynucleotide kinase based on a MnO_2 nanosheet-3,3′,5,5′-tetramethylbenzidine (TMB) colorimetric system. Anal Methods 8:4119–4126
26. Zhai W, Wang C, Yu P, Wang Y, Mao L (2014) Single-layer MnO_2 nanosheets suppressed fluorescence of 7-hydroxycoumarin: mechanistic study and application for sensitive sensing of ascorbic acid in vivo. Anal Chem 86:12206–12213
27. European Commission (2006) Regulation (EC) No. 1881/2006: Off. J. Eur. Union, 255, 14–17
28. Tang Y, Lai W, Zhang J, Tang D (2017) Competitive photometric and visual ELISA for aflatoxin B_1 based on the inhibition of the oxidation of ABTS. Microchim Acta 184:2387–2394